Acoustic Emission Based Deep Learning Technique to Predict Adhesive Bond Strength of Laser Processed CFRP Composites

Ramkumar Sathiyamurthy
Assistant Professor
Department of Mechanical Engineering
Aalim Muhammed Salegh
College of Engineering,
Chennai, Tamilnadu,
India

Muthukannan Duraiselvam
Professor
Department of Production Engineering
National Institute of Technology-
Tiruchirappalli,
Tamilnadu,
India

Sevvel P
Professor
Department of Mechanical Engineering
SA Engineering College,
Chennai, Tamilnadu,
India

The high degree of inhomogeneity in material and intricacies created by machining of carbon fiber reinforced plastic (CFRP) composites hinder the accurate prediction of residual strength of the adhesive bond joint using analytical models. Recently, artificial intelligence techniques are effectively utilized as an alternative method for predicting the results of complex phenomena. In this paper, attempts were made to predict the bond strength of laser surface treated and adhesively bonded CFRP composite specimens using the artificial neural network (ANN) from the acoustic emission (AE) parameter recorded during the shear test. Twelve adhesively bonded specimens whose surfaces were pre-processed with 3W Nd:YAG laser at different processing parameters. ANN was trained using segregated AE data according to the failure mechanism and the percentage of failure load (5 to 100%). Predicted values were compared with experimental values and the results were analysed for the suitability of ANN with AE in the application.

Keywords: *Acoustic emission, NDT, neural network, prediction, failure characterization.*

1. INTRODUCTION

Aviation and space industries were always in thirst of reliable and sustainable material for the better performance of their products [1]. CFRP composites are the ideal choice due to their superior mechanical properties like high tensile strength, good strength to weight ratio, radar absorption, water resistance and better impact resistance [2]. CFRP composites are widely utilised in critical components of advanced aerospace applications like helicopter rotor blades, fighter jet nose cone, wind turbine blades and robotic manipulators [3,4,5]. Due to its macroscopic inhomogeneity, it creates unique technological challenges while joining.

Adhesive bonding is preferred for a composite because of its distinct advantages like high fatigue strength and the lowest possible addition of weight [6]. In order to realise a good adhesive bond, the impregnated fibers should be made to expose out from bulk material prior to bonding. Because the outer matrix (epoxy) layer, being a binding element, will not bear any load and inherit the impurities from its manufacturing processes like grease, release agent and atmospheric dust and moisture. These difficulties nessaciate surface preparation prior to bonding and it will also improve the adhesive bonding strength by inducing roughness and wettability [7]. Laser surface processing being a non-contact type and ability to precisely adjust the process parameter makes it a distinct candidate for the pre-treatment of CFRP composite [8]. Because of its high power density, matrix element will be evaporated and leaving the fibers unaffected by selecting appropriate processing parameters. Oliveria et al.[9] results depicted that the change in surface morphology of fibers by laser radiation can affect the bond strength. Recently, Sathiyamurthy et al. [10] experimentally proved that even a micron level change in the surface characteristic of laser processed specimens can deteriorate the bond strength of CFRP composite to a higher extent.

The interaction of laser energy on CFRP composite is a complex phenomenon that makes it difficult to predict the surface morphology [11,12]. Predicting the final bond strength from the failure mechanism will pave the way to monitor a product in service and exploit it with confidence. Finite element analysis (FEA) was performed by Garinis et al. [13] for dynamic analysis of composite rotor blade and Dinulovic et al. [14] developed a novel Pan's theory based FEA model to predict mechanical properties of composite structures. Due to the complex failure behaviour of the composites, mathematically calculating the final bond strength is a challenging task and needs extensive computational infrastructure. These reasons necessitate the need for a simple and reliable expert system.

In recent times, deep learning, due to its simple mathematical operation and ability to fit the complex model, plays a vital role in various engineering domains, by learning the given problem and stating a more generalized result with acceptable error margin [15]. Simplest ANN will comprise three layers, namely input layer, hidden layer and output layer. Each neuron in a layer will be associated with every neuron in the succeeding layer through a communication link. The signal processed in a neuron will be transmitted to the adjacent

Received: December 2019 Accepted: May 2020
Correspondence to: Muthukannan Duraiselvam
Dept. of Production Engineering, National Institute of Technology – Tiruchirappalli, Tamilnadu, India.
E-mail: durai@nitt.edu
doi: 10.5937/fme2003611S

layer after it gets added with weight of the particular neuron and amplified by an activation function. Prediction accuracy of ANN relies on the learning algorithm, network size, data set and activation function [16]. Typical ANN structure is shown in figure 1.

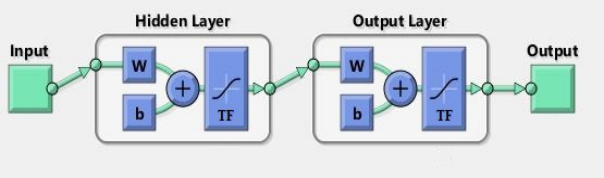

Figure 1. Simple artificial neural network. (w – weight, b – Bias and TF – transfer function).

AE technique is the method of detecting the sound wave generated while the failure of a specimen and characterising the sound to a particular phenomenon of activities occurred inside the material [17]. A typical AE signal is shown in figure 2.

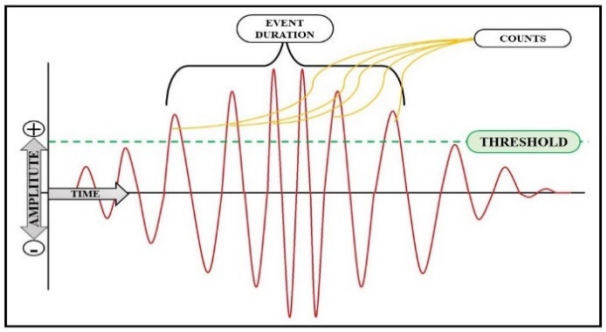

Figure 2. A typical AE signal.

Many researchers were attempted to characterise the failure mechanism by classifying AE signals amplitude collected during failure of composites. Berthelot and Rhazi [18] state that high amplitude signals belong to fiber failure and low amplitude signals are from matrix microcracking and debonding. Other researchers classified few amplitude ranges in between and associated it with corresponding failure mechanism [19-22]. Gong et al. [23] stated five failure types and distinguished it separately. Many studies were published using the combination of AE parameters with soft computing technique. Walker [24] predicted the failure strength of CFRP specimen using low amplitude signals and reported 3.74% error as a worst-case prediction. While other researchers reported the use of ANN in predicting the failure loads of composite specimens and reported prediction error up to two percentage [25-27].

2. MATERIALS AND METHODS

Unidirectional (0^Olayup) CFRP specimens were produced using a hot press process as a sheet of 35cm × 35 cm using 5 plies of unidirectional carbon fiber sheets each with a weight of 220gms/m^2. Commercially available epoxy and accelerator were used. Mould was kept in hot press for 1 hour at 5 bar pressure and 150^{o}C for curing as per the manufacturer recommendation and placed at room temperature for 48 hours for further curing. Samples as per ASTM-D5868 were marked and cut removed using a diamond edge cutter and edges were polished. Specimen dimensions are shown in figure 3.

Laser surface treatment was performed on both the specimens one surface, using a 3 Watts (average power) Nd:YAG laser working at 20KHz emits a 532nm wavelength and 0.15mJ constant pulse energy. Laser beam produced was linearly polarized (TEM_{00}) Gaussian beam with a diameter of 90µm. Galvo scanner with a scanning range of 100mm×100mm and resolution of 0.1 µm was used to scan the beam parallel to fiber orientation.

A single R15 AE sensor of 150kHz, the resonant type was used with a preamplifier of 35dB gain. AE data were processed and recorded using a Physical Acoustic Corporation DiSP AE system. Using an adhesive tape AE sensor was fastened 20mm below the width of the adhesive-bonded. Silicon vacuum grease was applied in the interface between sensor and specimen to reduce the transmission loss. By assessing the surrounding noise level, 35dB was fixed as a threshold limit. In order to In order to assure the operationality of AE system, pencil break test was conducted prior to the start of every experiment. Instron-5582 universal testing machine having a capacity of 100kN was used to load the bonded specimens until complete fracture at 5kN/min. Data obtained from specimens which broke only on the adhesive bonded joints were considered for the study. ANN was programmed using MATLAB-16 software. Schematic of the laser processing mechanism is depicted in figure 4.

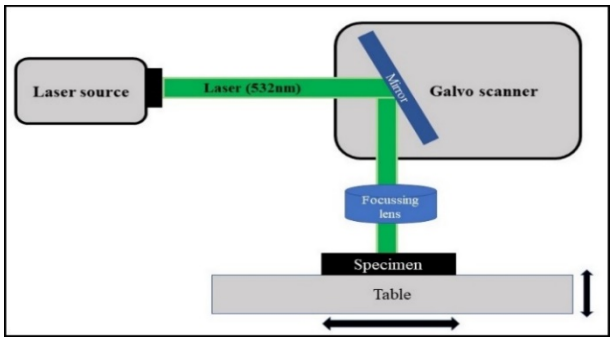

Figure 3. Specimen dimensions as per ASTM-D5868.

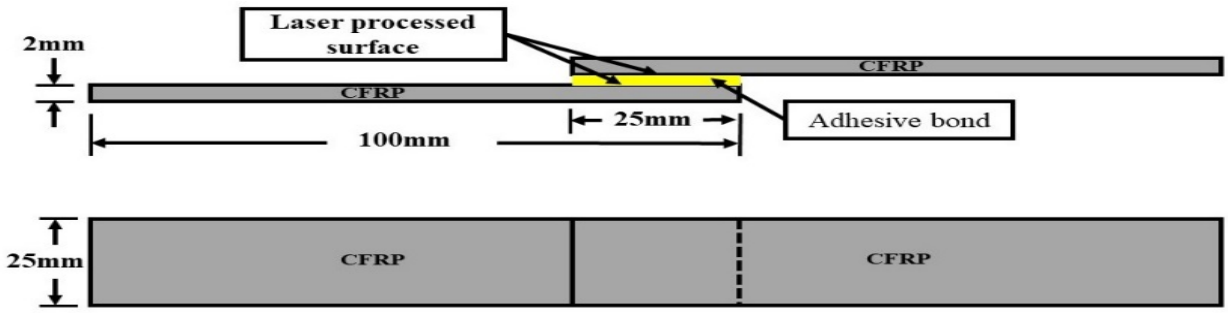

Figure 4. Schematic of laser processing mechanism.

3. RESULTS AND DISCUSSIONS

3.1 Laser Processing

CFRP composite specimens were processed by varying scanning speed, number of passes and percentage beam overlap in order to create different surface roughness. Specimens which are having only matrix ablation and different roughness values were considered for the study. Table 1 provides details of laser processing parameter, adhesive bond strength and roughness values.

Table:1. Laser processing parameter and adhesive joint properties. (A-scanning speed (mm/sec), B-percentage beam overlap and C-number of passes)

Specimen no.	A	B	C	Failure strength (MPa)	Rz (µm)
1	16	10	1	698	17.78
2	16	10	5	670	22.09
3	16	30	3	690	18.49
4	16	50	5	665	24.22
5	20	10	1	650	9.45
6	18	10	3	715	12.05
7	18	30	3	735	14.08
8	18	30	5	688	18.59
9	20	10	5	695	11.22
10	20	30	3	672	10.05
11	20	50	1	680	10.87
12	18	50	3	710	16.22
13	16	50	1	680	20.45
14	20	50	5	710	11.78

Scanning speed was varied between 16 mm/sec and 20mm/sec in step of 2mm/sec. The generated laser beam, due to the gaussian characteristics (TEM_{00}) will lack an energy density in the outer 10% of the beam diameter. So, the minimum beam overlap was assigned to 10% and the maximum was fixed to 50% to cover the full half of the distribution. After each number of passes surface roughness was measured using white light interferometry (WLI) technique and found no considerable increase in surface roughness after five number of passes. This is due to the fact that carbon fiber because of its high thermal conductivity, absorbs the laser energy and making it unable to penetrate further deep to create craters. So, maximum number of passes were fixed to five. With all these limits, experiment was designed using central composite design method in Minitab software.

Figure 5 shows the WLI surface profile of specimens number 4 and 5, which is having highest and lowest roughness respectively. Specimen number 4 (figure 5-a), due to the increased number of passes (5 nos.), lowest scanning speed (16mm/sec) and extreme beam overlap (50%), much of the matrix element (epoxy) was ablated due to high heat input. Which leads to a deep craters between fibers, thus creating higher roughness of 24.22µm. It can be visualized from the deep valley and hills in 2D roughness plot (figure 5-c). Specimen number 5, which delivered the lowest roughness of 9.45µm prior to bonding, shows a bare fiber on the surface (figure 5-b) with moderate groove depths (figure 5-c) due to very low heat input from the process.

3.2 Failure mode analysis

AE data were acquired during loading of specimens until complete fracture. According to literature, there are five modes of failure mechanism in composites namely matrix microcracking, delamination growth, fiber /matix decohesion, fiber/matrix pullout and fiber failure. Delamination type failure mode is rare in unidirectional fiber composites [16] but in case of adhesion bond, it will play a crucial role.

Since the stress generated due to applied load will be transferred through the joint, delamination activity in the bonded area will deteriorate the joint performance. Collected AE data consist of a wide range of hit counts from amplitudes ranging from 35dB to 120dB. Gong et al. [21] model of AE classification was utilized in this study.

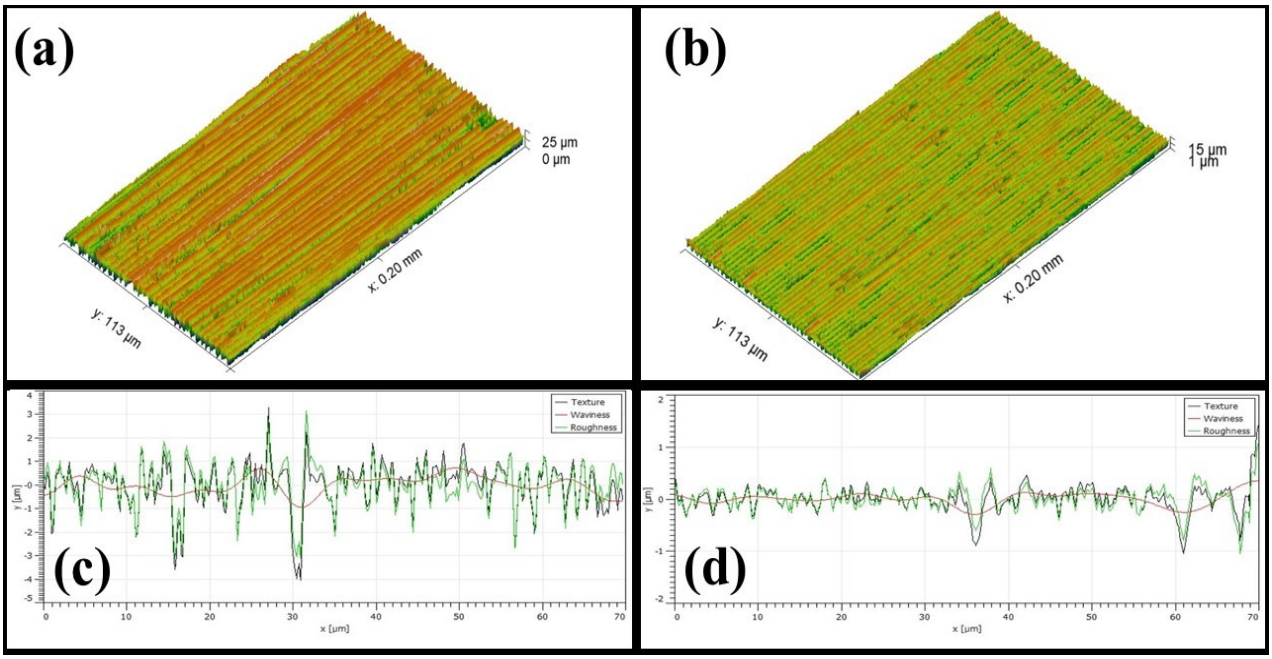

Figure: 5. WLI surface profiles (a) specimen 4 and (b) specimen 5. 2D roughness profile (c) specimen 4 and (d) specimen 5.

According to the AE classification model, matrix microcracking, delamination growth, fiber/matix decohesion, fiber/matrix pullout and fiber failure are associated with signals with an amplitude range of 33 – 45dB, 46 – 58dB, 59 – 68dB, 69 – 86dB and above 87dB respectively.

AE data generated while the failure of specimens was stored in a computer. Hit counts were segregated and summated according to the failure type up to the various percentage of failure load. Since no AE activity was recorded until five percentage of load, signals were segregated from five percentage to full load in the interval of five percent up to thirty percent and thereon increased to ten percent. In order to unveil the failure mechanism, specimens numbered seven and five which are on the extremity of failure load (750MPa and 650MPa respectively) were compared.

By comparing both the graph on figure 6. The microcrack formation was initiated very earlier for specimen 5 and started growing at a steady pace. Whereas for specimen 7 microcrack started to grow after 5% and saturated after 70%.

Similarly, delamination growth travelled in tandem with the generated microcracks, which is the main reason for the poor performance of specimen five. But in specimen seven microcracks generated in a gradual manner and the delamination grown at a very low pace until sixty percentage and thereafter it started to grow faster.

Fiber breakage which is the main reason for poor joint strength started to occur in very early stage (10%) in specimen-5, whereas in specimen-7 it started at forty percentage. Due to the fact that the fiber breakage signal count recorded for specimen-7 was much higher, it endured a much higher load than the other. In specimen-7 due to the slow growth rate of delamination, fiber was holding the load and starts to fail after fifty percentage of load, which is proven by the increased activity of fiber/matrix decohesion. In the final stage of failure, both specimens (after 90% of load) emitted higher counts of fiber breakage and fiber pull-out signal. SEM images of both the specimens interface were investigated after failure. Figure 7 shows the SEM image of fractured specimens. Lower bond strength of specimen 5 was due to the growth of microcracks and its penetration into the bond interface. The penetrated microcracks created delamination, which leads to the occurrence of debonding and fiber pullouts. The presence of delamination flakes and fiber pullouts in SEM image (figure 7-b) confirms the AE interpretation discussed above.

In contrast to specimen-5, specimen-7 shows no sign of excessive microcracks or fiber pullouts and shows heavy fiber fractures, this may be attributed to optimal interlocking between fibers and matrix. Better interlocking in specimen 7 is proven by the delayed start of fiber breakage (after 40%) and low count of fiber/matrix pullout. Also, it can be noted from the graph of specimen 7 (figure 6) that when ever the fiber breakage starts to accelerate, the fiber pullout curve is getting flattened. Only at the last stage of failure both the specimens exhibit fiber breakage accompanied by massive fiber pullouts, which is a natural phenomenon.

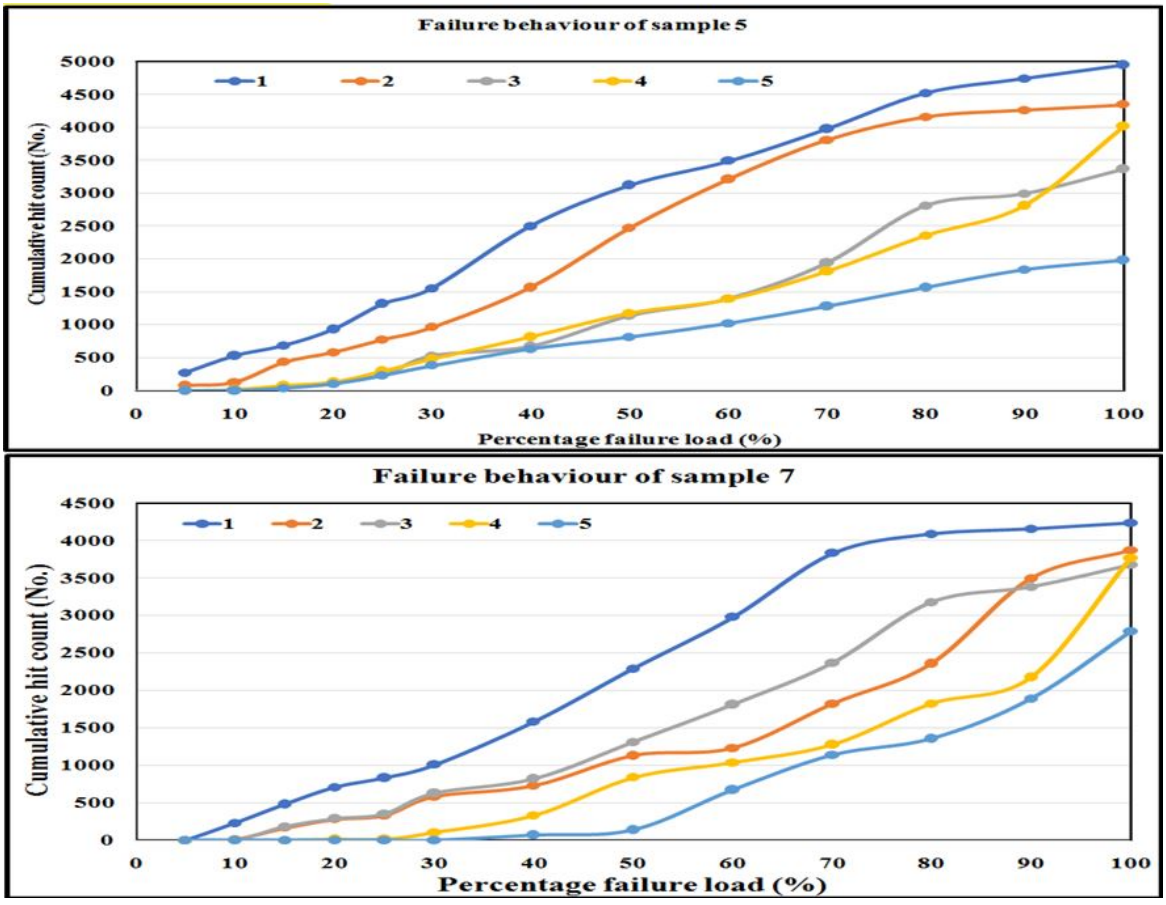

Figure 6. Cumulative hit count until failure. (1–matrix microcracking, 2–matrix/matrix friction or delamination growth, 3–interface decohesion or fiber/matrix decohesion, 4–fiber/matrix pullout and 5–fiber breakage).

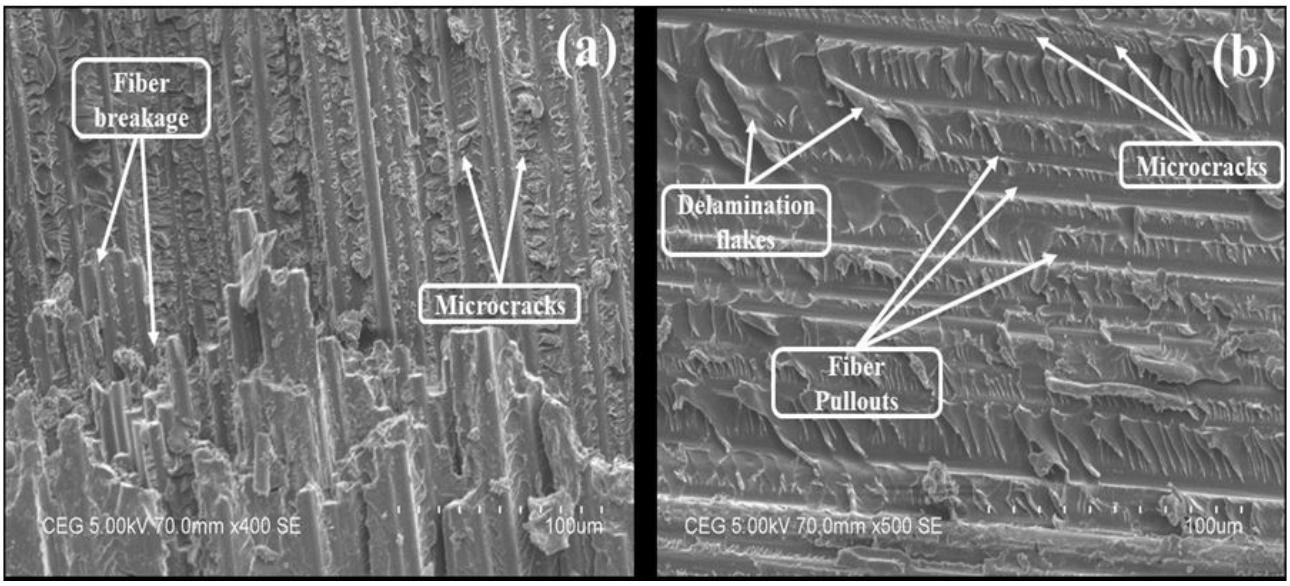

Figure 7. SEM Image of (a) Specimen 7 and (b) Specimen 5.

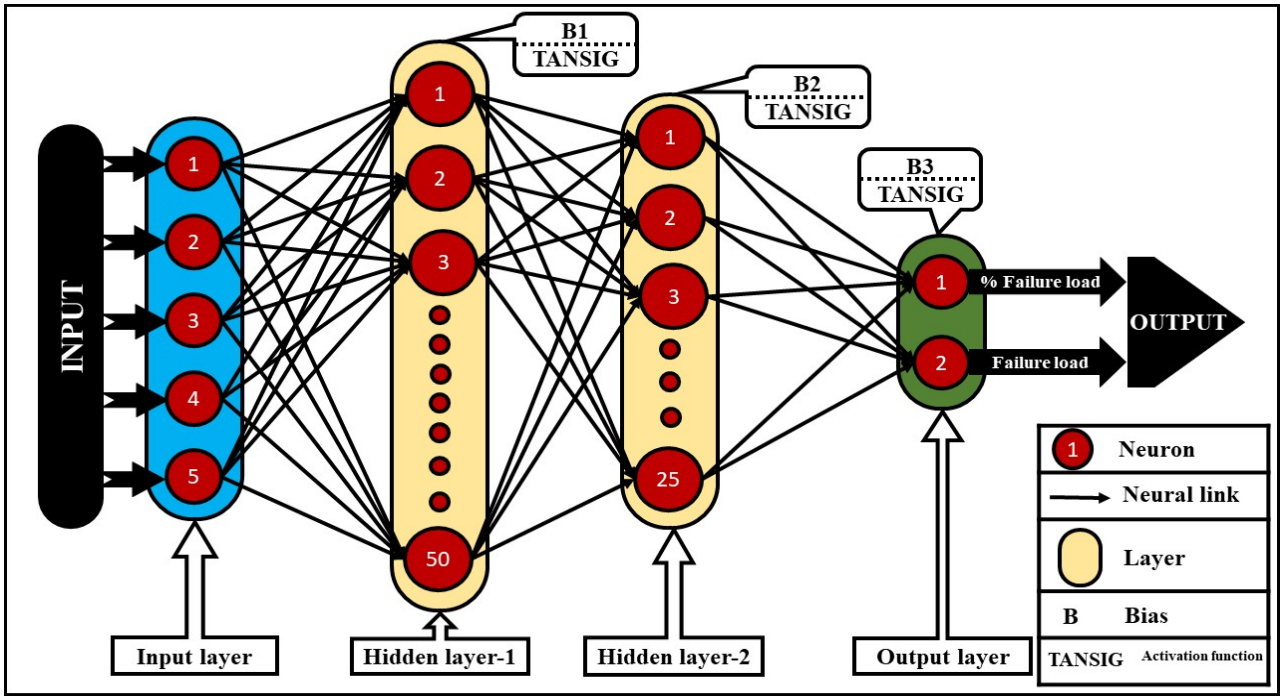

Figure 8. Schematic representation of ANN used for prediction.

3.3 Artificial neural network

AE data collected were segregated according to the five failure mechanism with respected to various percentages of failure load for all twelve specimens. So the input layer of ANN consist of five neurons, that is one neuron each to process data of each failure mechanism at the corresponding percentage of the load. In the real-life condition, two parameters are necessary to ensure the reliability and safety of the structure in service. First is the expected failure load and the second is anticipated residual strength. Both the parameters were accommodated inside ANN by providing two neurons in the output layer, one each for predicting the current percentage of load consumed and another for final failure strength.

In order to reduce the time of training, supervised training method was used. Supervised training of neural network needs two sets of data one for training and another for testing. Training data set will consist of both input and the corresponding exact output, but the testing set will consist only of the input and the network will be made to predict the output. Data of specimens three, four and six due to the varied failure strength were selected for testing and the output will not be shared with the ANN. Further, the training set was divided into three sets namely training (75%), testing (15%) and validation (10%) for the better convergence. Training data set will be randomized before feeding into the ANN.

Supervised learning needs a special backpropagation mechanism to alter the weights and biases for better prediction. Levenberg-Marquardt algorithm being the fastest backpropagation algorithm was deployed to improve the learning rate of ANN. Various network dimensions were tested by altering all the network parameters (number of neurons, number of hidden

layers and activation function). The number of neurons per layer was limited to hundred due to computational limitation and to conserve convergence time. Network dimension of 5-50-25-2 (Input layer – Hidden layer 1 – Hidden layer 2 – Output layer) predicted the testing data with better accuracy. Schematic layout of the network is shown in figure 8.

Better performance was achieved at 1303rd iteration after which the training stopped due to the increase in a validation error. The convergence plot for the network is shown in figure 9. ANN fitted the entire data set for training (training, validation and testing data sets) with better accuracy as shown in the regression plot (figure 10). The initial learning rate (momentum) was fixed to 0.00001. The network was allowed to decrease momentum at the rate of 0.001 when moving down and increase the momentum to 5 when moving uphill. Maximum validation fails were permitted for six iterations after which the network will stop learning.
Prediction of the network for the data of three untrained specimens for the percentage of load and final failure load is depicted in figure 11.

Prediction of the network for percentage failure load was very turbulent below forty percentage, after which the accuracy was within five percent mark. The same trend was followed in failure strength prediction also. Failure load prediction of ANN for the three specimens was provided graphically in figure 12. Especially at five percentage, the prediction was very poor. This is due to the fact that the AE activity at five percentage was more or less similar to all the specimens and below forty percentage was less distinguishable. So the ANN was unable to predict with much accuracy.

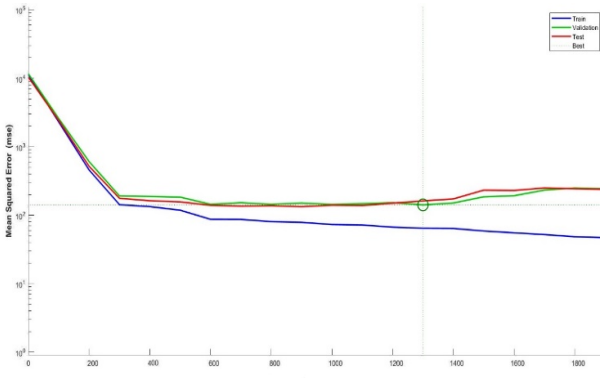

Figure 9. Convergence plot

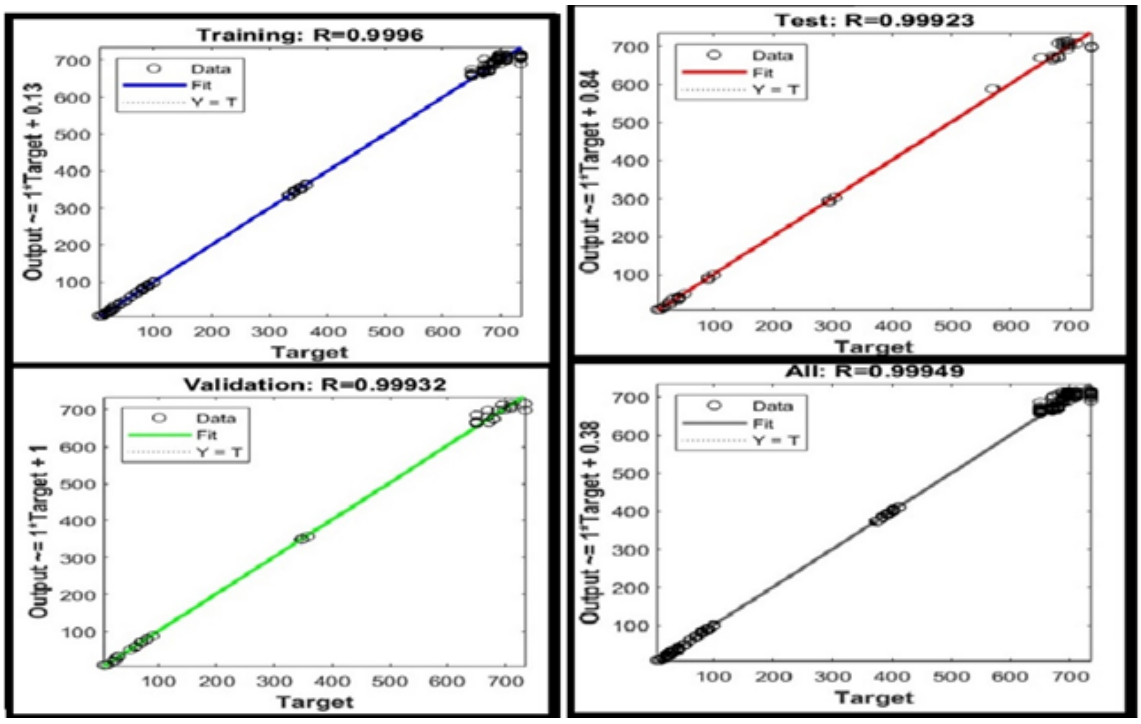

Figure 10. Regression plots

4. CONCLUSION

Laser processed and adhesively bonded CFRP specimens with different surface roughness were tested mechanically for joint strength. Failure mechanisms were analysed with a real-time acoustic emission technique. Supervised learning type artificial neural network was designed and trained to predict the percentage of failure load deteriorated and its full failure load using AE data. From the results following conclusions were drawn:

- Segregation of AE data according to failure modes yields better results in ANN simulation.
- ANN with the structure of 5-55-25-2 predicted the percentage failure load and failure strength more accurately.
- Accuracy of prediction for percentage failure load was more accurate and precise above the 40% load.
- Accuracy of prediction for percentage failure load was neither accurate nor precise below 40% of load and varies from 41% to 8% error.
- Final failure load was predicted with great accuracy of 3.5% to 0.1% error margin.
- Thus ANN coupled with AE monitoring can be used as an efficient and effective tool for real-time health monitoring of CFRP composite structures.

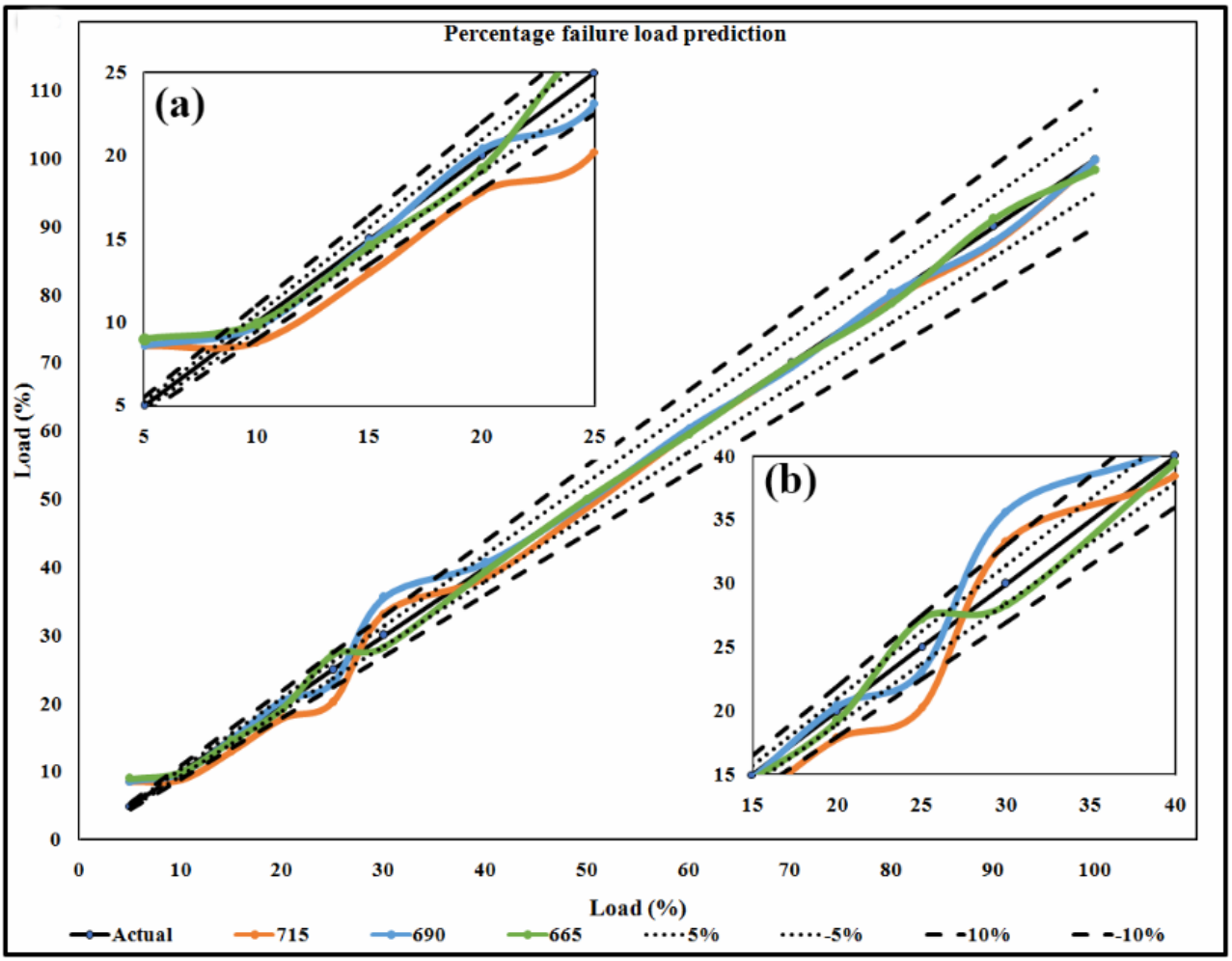

Figure 11. Percentage failure load predicted. Magnified view of (a) 5 to 25% load and (b) 15 to 40% load.

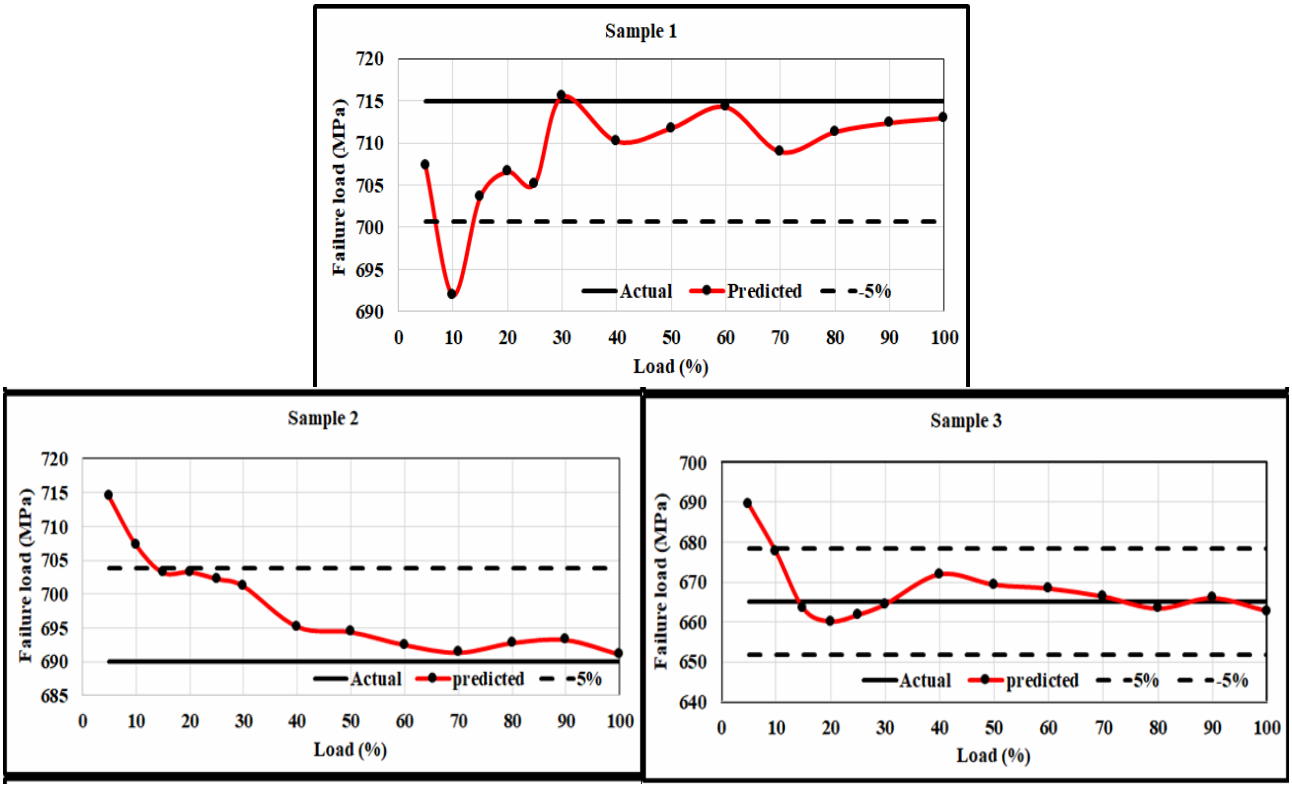

Figure 12. Failure load predicted by ANN for different Samples.

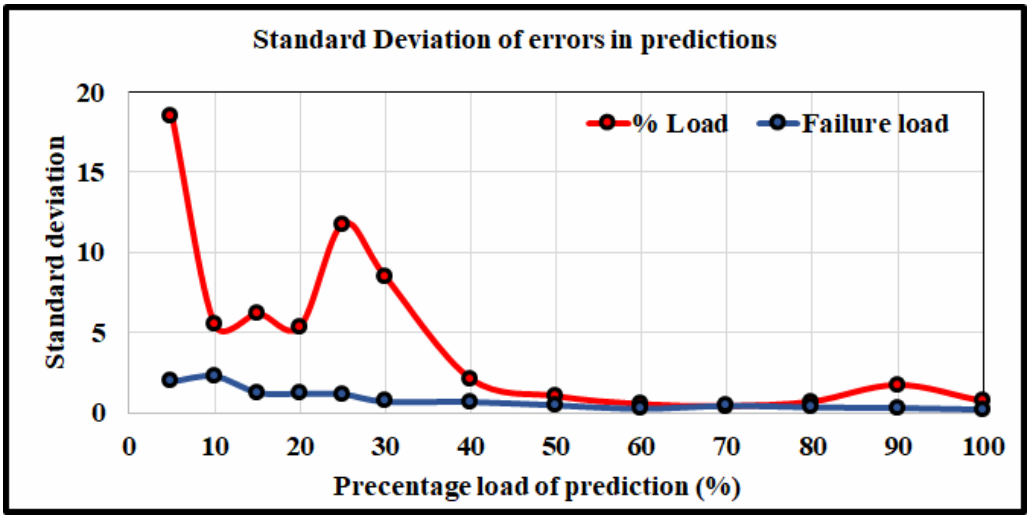

Figure 13. Standard deviation in prediction errors.

REFERENCES

[1] Jawaid, M. and Thariq, M.: Handbook Sustainable Composites for Aerospace Applications, Woodhead Publishing - Elsevier, Cambridge, 2018.

[2] Zweben, C.H., Beaumont. P.W.R.: Comprehensive Composite Materials II, 2nd Edition, Elsevier Ltd., Amsterdam, 2018.

[3] Rasuo B.: Aircraft production technology. Belgrade: Faculty of Mechanical Engineering, 1995.

[4] Kumar, S.H.S., Anand, R.B.: A case study on damage detection of wind turbine composite blade, FME Transactions, Vol. 47, pp. 135-141, 2019.

doi: 10.5937/fmet1901135S

[5] Karthikeyan, P., Sabarianand, D.V., Suganthan, S.: Investigation on adaptability of carbon fiber tube for serial manipulator, FME Transactions, Vol. 47, pp. 412-417, 2019.

doi: 10.5937/fmet1903412K

[6] Beaumont, P.W.R., Soutis, C. and Hodzic, A.: Structural integrity and durability of advanced composites: Innovative modelling methods and intelligent design, Woodhead Publishing - Elsevier, Cambridge, 2015.

[7] Wegman, F.R., Twisk, J.V.: Surface preparation techniques for adhesive bonding, William Andrew – Elsevier, Oxford, 2013.

[8] Mishar, D.R., Gautham, G.D., Prakash, D., Bajaj, A., Sharma, A., Bisht, R., Gupta, S.: Optimization of kerf deviations in pulsed Nd:YAG laser cutting of hybrid composite laminate using GRA, FME Transactions, Vol. 48, pp. 109-119, 2020.

doi:10.5937/fmet2001109M

[9] Oliveira, V., Sharma, S.P., de Moura, M.F.S.F., Moreira, R.D.F., Vilar, R.: Surface treatment of CFRP composites using femtosecond laser radiation, Optics and Lasers in Engineering. Vol. 94, pp. 37–43, 2017. https://doi.org/10.1016/j. optlaseng.2017.02.011

[10] Sathiyamurthy, R., Duraiselvam, M.: Selective laser ablation of CFRP composite to enhance adhesion bonding, Materials and Manufacturing Processes. Vol. 34, pp. 1296–1305, 2019. doi:10.1080/10426914.2019.1644453

[11] Gautam, G.D., Mishra, D.R.: Evaluation of geometrical quality characteristics in pulsed Nd: YAG laser cutting of Kevla-29/Basalt fiber reinforced hybrid composite using grey ralational analysis based on genetic algorithm, FME Transactions, Vol. 47, pp. 560-575, 2019. doi:10.5937/fmet1903560G

[12] Ali, H.T., Fotouhi, S., Akrami, R., Pashmforoushd, F., Pavlovic, A., Fotouhi, M.: Effect of ply thickness on damage mechanisms of composite laminates under repeated loading, FME Tansactions, Vol. 48, pp. 287-293, 2020. doi:10.5937/fme2002287T

[13] Garinis, D., Dinulović, M. and Rašuo, B.: Dynamic Analysis of Modified Composite Helicopter Blade, FME Transactions, Vol. 40, No. 2, pp. 63-68, 2012.

[14] Dinulović, M., Rašuo, B., Krstić, B. and Bojanić, A.: 3D random fiber composites as a repair material for damaged honeycomb cores, FME Transactions, Vol. 41, No. 4, pp. 325-332, 2013.

[15] Kharwar, P.K., Verma, R.K.: Grey embedded in artificial neural network (ANN) based on hybrid optimization approach in machining of GFRP epoxy composites, FME Transactions, Vol. 47, pp. 641-648, 2019. doi: 10.5937/fmet1903641P

[16] Fausett, L., Fausett, L.V.: Fundamentals of Neural Networks: Architectures, Algorithms, and Applications, Prentice-Hall, 1994.

[17] American society for testing materials, ASTM-E1316. Annual Book of ASTM Standards; Vol. 3, 2019.

[18] Berthelot, J.M., Rhazi, J.: Acoustic emission in carbon fibre composites. Composites Science and Technology, Vol. 37, pp. 411–428, 1990. https://doi.org/10.1016/0266-3538(90)90012-T

[19] J.R. Wadim: Acoustic Emission Applications. Dunegan, San Juan Capistrano, 1978.

[20] Kim, S.-T., Lee, Y.-T.: Characteristics of damage and fracture process of carbon fiber reinforced

plastic under loading-unloading test by using AE method, Materials Science and Engineering: A. pp. 234–236, pp. 322–326, 1997. https://doi.org/10.1016/S0921-5093(97)00226-8

[21] Kotsikos, G., Evans, J.T., Gibson, A.G., Hale, J.: Use of acoustic emission to characterize corrosion fatigue damage accumulation in glass fiber reinforced polyester laminates, Polymer Composites. Vol. 20, pp. 689–696, 1999.

[22] Ceysson, O.; Salvia, M.; Vincent, L. Damage Mechanisms Characterization of Carbon Fiber /Epoxy Composite Laminates by Both Electrical Resistance Measurements and Acoustic Emission Analysis, Scripta Materialia, Vol. 8, Issue 34, 1996. https://doi.org/10.1016/1359-6462(95)00638-9.

[23] Chen O.; Karandikar P.; Takeda N.; Rcast T. K. Acoustic Emission Characterization of a Glass-Matrix Composite, Nondestructive Testing and Evaluation, Vol. 8, Issue 1, pp. 869–878, 1992. https://doi.org/10.1080/10589759208952759.

[24] X.L. Gong, A. Laksimi, M.L. Benzeghagh: New approach of the acoustic emission and its application to the identification of the damage mechanisms in composite materials, Revue des composites et des matériaux avancés. Vol. 8, Issue 1, pp. 179–205, 1998.

[25] Walker, J.L., Hill, E.V.K.: Backpropagation neural networks for predicting ultimate strengths of unidirectional graphite/epoxy tensile specimens, Adv Perform Mater, Vol. 3, pp. 75–83, 1996. https://doi.org/10.1007/BF00136861

[26] Caprino, G., Teti, R., de Iorio, I.: Predicting residual strength of pre-fatigued glass fibre-reinforced plastic laminates through acoustic emission monitoring, Composites Part B: Engineering, Vol. 36, pp. 365–371, 2005. https://doi.org/10.1016/j.compositesb.2005.02.001

[27] Bar, H.N., Bhat, M.R., Murthy, C.R.L.: Identification of failure modes in GFRP using PVDF sensors: ANN approach. Composite Structures. Vol. 65, 231–237, 2004.

ТЕХНИКА ДУБОКОГ УЧЕЊА БАЗИРАНА НА АКУСТИЧНОЈ ЕМИСИЈИ ЗА ПРЕДВИЂАЊЕ ЈАЧИНЕ АДХЕЗИЈЕ КОД ЛАСЕРСКИ ТРЕТИРАНИХ CFRP КОМПОЗИТА

Р. Сатијамурти, М. Дураиселвам, Севел П.

Висок степен нехомогености материјала и проблеми настали обрадом CFRP композита онемогућавају примену аналитичких модела за прецизно предвиђање заостале чврстоће везе добијене адхезијом споја. У новије време користе се технике вештачке интелигенције као алтернативни метод за предвиђање резултата ове сложене појаве. Рад приказује покушај предвиђања јачине споја код површине третиране ласером и адхезијом добијене везе код узорака CFRP композита коришћењем вештачке интелигенције на основу параметара акустичне емисије добијених испитивањем на смицање. Извршена је предобрада површине 12 узорака ласером 3W Nd:YAG при различитим параметрима обраде. Вештачка интелигенција је тренирана одабраним подацима добијеним акустичном емисијом на основу механизма отказа и оптерећења отказа (5 – 100%). Предвиђене вредности су упоређене са вредностима добијеним експериментом и извршена је анализа резултата у циљу утврђивања могућности примене вештачке интелигенције са акустичном емисијом.